Available online at www.CivileJournal.org

Civil Engineering Journal

(E-ISSN: 2476-3055; ISSN: 2676-6957)

Vol. 11, No. 07, July, 2025

Consolidation Behavior of Soft Soil Treated with PVDs and Vacuum-Surcharge Preloading

Nghia Trong Le [1, 2], Kien Trung Nguyen [1, 2*], Minh Trung Nguyen [1, 2]

[1] *Faculty of Civil Engineering, Ho Chi Minh City University of Technology (HCMUT), Ho Chi Minh City, Vietnam.*

[2] *Vietnam National University Ho Chi Minh City, Linh Xuan Ward, Ho Chi Minh City, Vietnam.*

Received 03 January 2025; Revised 04 June 2025; Accepted 11 June 2025; Published 01 July 2025

Abstract

Prefabricated vertical drain (PVD) combined with vacuum-surcharge preloading is a widely used ground improvement technique to accelerate the dissipation of excess pore water pressure and reduce the soil compressibility. However, difficulties in the numerical simulations of water dissipation and equivalent permeability of soil with PVDs in three-dimensional (3D) and two-dimensional (2D) settings cause substantial deviation of numerical results from observational data. Moreover, the optimum length of PVDs has not been well documented. Accordingly, this work analyzes a project in Dong Nai, Vietnam, where a 37-meter-thick soft soil was treated with PVDs and vacuum-surcharge preloading. In this work, the field observations and finite element method with consolidation theory were used to analyze the ground settlements, lateral displacements, and excess pore water pressure. The observed and simulated data shows that (i) the rate of settlements in the first 60 days of increasing preloading pressure is about 2.1 times faster than that in the next 110 days of constant preloading pressure, (ii) at 170 days, the ground-surface lateral displacement at the toe of the embankment is around 50 mm and reaches its maximum value of 150 mm at 1.55 m depth, and (iii) the dissipation of pore water pressure is closely correlated with the settlement rate. Moreover, back analysis indicates that a permeability conversion ratio from 1.872 to 4.538 should be applied to achieve the same degree of consolidation between 3D and 2D models. Lastly, the optimum length of PVDs in this project is 28 m, around 76% of the fully penetrated length into the soft layer.

Keywords: Water Dissipation; Settlement; Vacuum Preloading; PVD; Surcharge Preloading.

1. Introduction

The dissipation of excess pore water pressure (EPWP), also known as primary consolidation, is the process where water is squeezed out from a volume of fully saturated soil in response to an increase in effective stress [1]. This type of water movement leads to the settlement of soil foundation, which is a matter of the utmost importance in construction areas. The rate of pore water dissipation, i.e., the rate of ground settlement, depends primarily on the soil hydraulic conductivity (or the coefficient of permeability) [2]. For coarse-grained soils with high permeability, such as gravel and sand, the water can flow easily through the soil domain; thus, the settlement occurs almost immediately after increasing effective stress. On the contrary, for fine-grained soils with low permeability, such as silt and clay, it takes months or years for the soil to reach the primary consolidation settlement. The excessive consolidation settlement of this low-permeability soil frequently results in foundation failures, cracking, tilting, and damage in engineering structures, ruptures in underground pipeline systems, and so on [3]. It is, therefore, important to investigate the water dissipation and settlement in construction areas to assess the risk and the integrity of the structural systems.

* Corresponding author: nguyentrungkien@hcmut.edu.vn

http://dx.doi.org/10.28991/CEJ-2025-011-07-024

Prefabricated vertical drain (PVD) is one of the most cost-effective approaches to accelerate the consolidation stage of clayey soils by increasing the overall hydraulic conductivity. The wick drains are usually combined with vacuum pressure and/or surcharge loading to increase soil bearing capacity and reduce post-construction settlement. This combination treatment has been widely used for large projects, such as metro depots, airports, resorts, roads, and embankments [4-9].

Researchers have paid much attention to the analyses of water dissipation and settlement in construction areas with PVDs and vacuum-surcharge preloading. The pioneer studies, initially proposed by Barron [10] and later extended by Hansbo [11], developed the concept of cylindrical unit cell with radiational consolidation theory. Recently, Shen et al. proposed a diameter reduction method to include smear effect based on Hansbo's solution [12]. However, the unit cell solution and its variant were obtained using an assumption of zero lateral displacement, which is only applicable to the PVDs at the center of the projects. For those located near the edges of the structures, or at the toes of the embankments, lateral displacements are significant, and the unit cell solution may not be appropriate. Moreover, there are normally thousands of PVD in an engineering project, making the simulation of all individual unit cells a cumbersome process. Subsequently, aiming for convenience of plane strain modeling using the finite element method (FEM), many studies have proposed approaches to transform the axisymmetric unit cell into an equivalent two-dimensional (2D) model. Hird et al. used a matching procedure of geometry and permeability to convert an axial symmetry unit cell into a plane strain condition [13]. Meanwhile, Indraratna et al. transformed axisymmetric into plane strain configurations by adjusting the soil permeability and applied vacuum pressure [14]. Later, Parsa-Pajouh et al. performed a back analysis from three case studies to determine the coefficient of permeabilities for axisymmetric and plane strain simulations of PVDs [15]. Although the plane-strain model is practical, its results often deviate from observational data [16]. Also, the plane-strain model encounters difficulties in mesh complexity, in which a very dense FEM mesh is required at the narrow width of the drain. Recently, with the aid of numerical packages, such as PLAXIS and FLAC, 1D drain elements with zero thickness have been incorporated into numerical models to represent the PVDs and their surrounding zones [15, 17, 18].

Another challenge for geotechnical engineers lies in the determination of optimum length for the PVDs. Partial penetration may cause insufficient drainage, while full penetration into thick clayey layers may become uneconomical and cause leakage of vacuum pressure in two-way drainage [19, 20]. There exists an optimum length of PVDs where the partially penetrated PVDs accelerate the consolidation of soft soil as much as the fully penetrated PVDs do [20]. Nevertheless, only a few studies have dealt with this problem. Chai et al. proposed a simplified method to calculate the optimum penetration of PVDs in two-way drainage soil profiles [9], in which the horizontal water flow and progressive dissipation of pore pressure are ignored. Lately, Vu developed a method based on differential evolution and constraint-handling technique to find the optimal length and spacing of PVDs in multilayered soil profiles, although a computational subroutine was required for the algorithm and the results were not validated with other studies [21]. Meanwhile, Chen et al. analyzed a case study of a soft clay deposit improved by PVDs and used FEM to determine the effective depth of the drains based on the degrees of consolidation [22].

As previously mentioned, there remain difficulties in accurately predicting soil settlement, water dissipation, and optimum length of vertical drains in the PVD-treated soft soils. This study presents 3D and 2D plane-strain FEM simulations of a soft soil medium treated with PVDs and vacuum-surcharge preloading at a port project in Vietnam. The behavior of soft soil was governed by the Soft Soil Creep model. The 3D model was initially validated with field observational data and subsequently used to investigate the ground settlement, lateral displacement, and EPWP. Besides, back analyses were conducted with the field data to derive an equivalent permeability conversion ratio for the simulation of PVD-treated soil in 2D plane-strain problems. Moreover, the optimum penetration of PVDs into the soft soil layer was determined by analyzing the ground-surface settlement results from 2D simulations.

The remainder of this paper is organized as follows: Section 2 describes the project used in this study. Section 3, meanwhile, presents the consolidation theory and numerical modeling of the problem. In Section 4, the field data and simulated results are used to analyze the ground settlements, lateral displacement, and EPWP. The equivalent permeability conversion ratio and optimum length of PVDs in 2D plane-strain models are also derived in Section 4. The concluding remarks are provided in Section 5.

2. Project Description

The "Phuoc An Port and Logistic Zone" project is located in Nhon Trach district, Dong Nai province, Vietnam. In this project, a 29-hectare area of soft soil was treated with PVDs and vacuum-surcharge preloading to ensure a sufficient soil bearing capacity for operational loads, such as containers and local traffic [23]. This study analyzes the 9170 square meter zone C1, the area enclosed by the red line as shown in Figure 1. The design load is taken as 20 kN/m², while the consolidation is required at 98%, and the settlement after 20 years is expected within 30 to 70 cm.

Figure 1. The "Phuoc An Port and Logistic Zone" project and zone C1 (*https://www.portcoast.com.vn/projects/phuoc-an-port-and-logistic-zone*)

From the original surface, the soil profile at zone C1 consists of around 37 m thick very soft to soft clay, underlain by a layer of medium-dense clayey sand [24]. The natural water content varies from 80% in soft clay to 120% in very soft clay, while the void ratio remains relatively unchanged around 2.0. The N-SPT values are almost zero throughout the 20 m upper part and increase gradually to the value of N = 7 at the bottom of the clay layer. The dissipation of EPWP in this soft soil layer was accelerated by a system of PVDs with cross-section dimensions of 0.004 m × 0.1 m and a length of 35 m. The PVDs were installed in a square pattern with a center-to-center spacing of 1.0 m.

Regarding instrumentations, settlement plates, extensometers, and piezometers were installed at the center of zone C1 to measure surface settlement, sub-surface settlement, and pore water pressure (PWP), respectively. The sub-surface settlement was recorded at the depths of -4.8 m, -14.4 m, and -24.4 m, while PWP was measured at the depths of -5.5 m, -15.5 m, and -25.5 m.

Vacuum suction and surcharge were used to preload the construction site. The treatment pressure is a sum of the vacuum pressure and the weight of sand used as surcharge. The histories of treatment pressure and surcharge height are shown in Figure 2. Around two months after the surcharge, a vacuum pressure of 70 kPa was applied and monitored during the preloading process to ensure a proper treatment. It took time for the vacuum to be stable around 70 kPa, and this work analyzes the construction site in the subsequent period of nearly 170 days with settlements recorded.

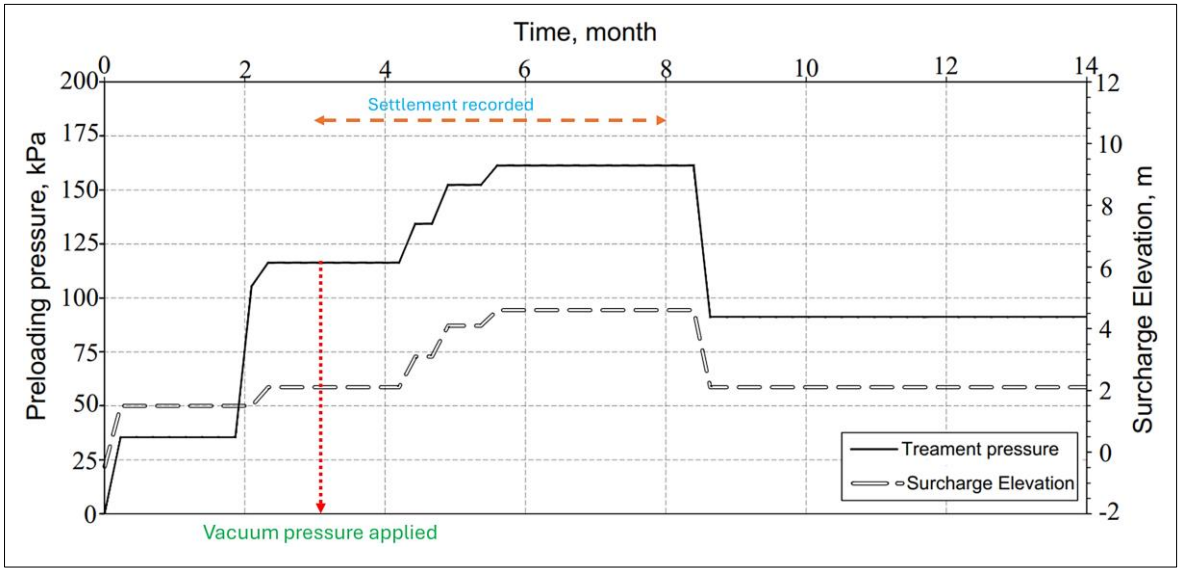

Figure 2. Time histories of treatment pressure and surcharge height

3. Research Methodology

The analysis was carried out using FEM implemented in PLAXIS software [25]. When it comes to the simulation of soft ground treated with PVDs, the water dissipation during consolidation process, the soil hydraulic conductivity, and the soil material model are the most important factors affecting the reliability of the numerical model.

3.1. Consolidation Theory and Finite Element Discretization

The consolidation is a coupling hydro-mechanical process, in which the groundwater flows in the porous soil medium. The governing equations of the consolidation process are based on Biot's theory [26], in which the water flow complies with Darcy's law and the soil skeleton is assumed to be elastic. The coupling characteristics are expressed via the equilibrium and continuity Equations [25]:

$$\begin{bmatrix} K & L \\ L^T & -S \end{bmatrix} \begin{bmatrix} \partial \underline{v}/\partial t \\ \partial \underline{p_n}/\partial t \end{bmatrix} = \begin{bmatrix} 0 & 0 \\ 0 & H \end{bmatrix} \begin{bmatrix} \underline{v} \\ \underline{p_n} \end{bmatrix} + \begin{bmatrix} \partial \underline{f_n}/\partial t \\ \underline{q_n} \end{bmatrix} \quad (1)$$

where $\underline{v}$, $\underline{p_n}$, $\underline{f_n}$, and $\underline{q_n}$ are the nodal displacement vector, nodal excess pore pressure vector, nodal load vector, and nodal vector prescribing the outflow at the boundary, respectively. In PLAXIS, the flow boundary can be simulated as closed boundary with zero flux, or open boundary with zero excess pore pressure. Meanwhile, K, L, S, and H are the stiffness, the coupling, the compressibility, and the permeability matrices, respectively.

It should be noticed that the nodal values of displacement and excess pore pressure are obtained by solving Equation 1. The values at the interior of the elements are interpolated by:

$$\underline{u} = N\underline{v}, \quad \underline{p} = N\underline{p_n} \quad (2)$$

where $\underline{u}$ is the displacement vector at a location within an element, $\underline{p}$ is the excess pore pressure, and N is the matrix of interpolation functions.

In Equation 1, the soil material constitutive model is included in the stiffness matrix K, while the soil hydraulic conductivity is assembled in the permeability matrix H. To be more specific, these matrices are calculated as:

$$K = \int B^T MBdV \ , \ H = \int (\nabla . N)^T k(\nabla . N)dV \quad (3)$$

where B is the strain interpolation matrix and M is the material stiffness matrix. The matrix k is assembled from the permeability k_x, k_y, and k_z along x, y, and z directions, respectively, as follows:

$$K = \begin{bmatrix} k_x & 0 & 0 \\ 0 & k_y & 0 \\ 0 & 0 & k_z \end{bmatrix} \quad (4)$$

3.2. Three-Dimensional Modeling

The behavior of soft soil with PVDs and vacuum-surcharge preloading was analyzed using FEM in 3D configuration. The 3D characteristic enables the numerical model to mimic closely the reality, including construction stages, elastic-plastic deformation, water dissipation and flow, PWP, stresses, and consolidation settlement. The soil domain is discretized using 15-node wedge elements, providing second-order interpolation of displacements. The PVDs were simulated using a line drain element. Noted that it is impossible to model vacuum as negative air pressure in PLAXIS. Instead, reducing the ground water head is a technique to imitate the vacuum consolidation. The groundwater head is reduced at the top free surface of the ground, and a fully coupled flow-deformation analysis is performed using this hydraulic boundary conditions. In such manner, 7.0 m reduction in water head corresponds to an equivalent vacuum pressure of 70.0 kPa. The 3D numerical model of the project is shown in Figure 3.

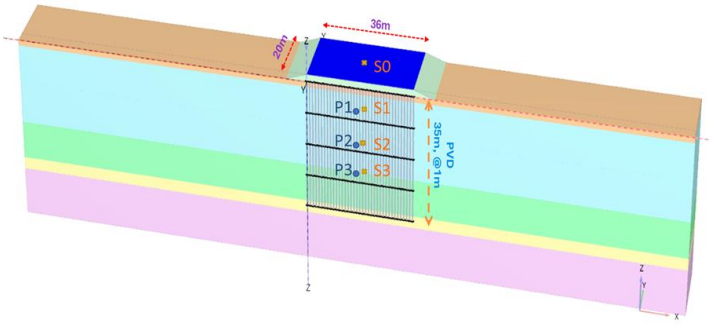

Figure 3. The 3D numerical model used for the analysis

The Isotropic Hardening Soil (HS) model was used to simulate the stress-strain relationship of two sand layers. In this advanced constitutive material model, the variation of soil stiffness is sufficiently represented using three different stiffnesses, namely the secant stiffness in standard drained triaxial test E_{ref}^{50}, the triaxial unloading/reloading stiffness test E_{ref}^{ur}, and the tangent stiffness for primary oedometer loading E_{ref}^{oed}. Besides, this material model is able to account for the stress-dependent stiffness using the power number m.

Empirical relationships between the Standard Penetration Test (SPT) N value and soil stiffness have been extensively investigated using experimental data from a wide range of soil types. For sandy soils, the ratio between elastic modulus and N varies from 2000 to 4000, depending on soil conditions and testing methods. The Architectural Institute of Japan suggests a ratio of 2800 as a representative parameter for geotechnical design [27]. In this study, a back-analysis was performed, and the value of E_{ref}^{50}/N was selected as 2200.

Meanwhile, the Soft Soil Creep model was used to govern the responses of the clayey layers. This model is capable of distinguishing primary loading and unloading-reloading, representing logarithmic compression behavior with a stress-dependent stiffness, and considering time-dependent creep settlement. The stiffness parameters of this material model are the compression index C_c, the swelling index C_s, and the creep index C_s. The soft clay was divided into three sublayers to better capture the variation of soil properties with depth.

The project site consists a thick layer of soft clay, extending to a depth of approximately 37 meters. Given the weak nature of this thick layer, the soil properties should be adequately determined to ensure the reliability of the calculated settlements. The input soil parameters for this model are obtained from laboratory tests. Specifically, 1D consolidation compression tests were conducted to determine the compression index C_c and swelling index C_s, which characterize the compressibility of clay. Besides, shear strength parameters, i.e. cohesion c' and internal friction angle φ', were obtained through consolidated undrained triaxial compression tests. On the contrary, the geotechnical investigation for the project did not include consolidation tests extending to the secondary compression stage to determine the secondary compression index C_α. In highly compressible clays, secondary consolidation settlement becomes more significant than it does in the case of over-consolidated clayey soils. Therefore, this study adopted the back analysis approach to achieve a reasonable value of C_α. The initial value of C_α was chosen based on the work of Mersi et al. [28], which is about $0.04C_c$. Although it is not presented here, iterative simulations were performed in which the value of C_α was calibrated to fit the field monitoring settlements. The value of C_α was eventually taken as $0.038C_c$.

The vertical permeability k_z of the soft clay was obtained from the 1D consolidation compression test. The lateral permeability of the untreated soil $k_x = k_y$ was calculated from the ratio k_x/k_z, which was reported in the range from 2 to 4 for clayey soil [29]. A value of $k_x/k_z = 2$ was taken in this study. For PVDs-treated zone, the soil permeability is affected by the disturbance during the PVDs installation process. According to the back-analyses, the field and lab tests in published work [30, 31], the lateral permeability is typically reduced by a factor of 2 due to smear effects.

The properties of the untreated soil layers used in the numerical model are summarized in Table 1. The soft clay layers were treated with PVDs installed in square pattern with the spacing of 1.0 m and the depth of 35 m. For the PVDs-treated zone of soft clay, the lateral permeabilities k_x and k_y are halves of those in untreated zones, while all other input parameters remain unchanged.

Table 1. The soil properties in the numerical models

Parameters	0. Backfill Sand	1A. Very soft clay	1B. Soft clay	1C. Medium soft clay	2. Sand, medium dense
Layer thickness (m)	1.5	21.9	10.3	3.3	13.0
Unit weight γ_{unsat} (kN/m^3)	18.0	15.3	15.3	15.5	20.2
Plasticity index PI (%)	0.0	46.9	45.0	43.4	0.0
Saturated unit weight γ_{sat} (kN/m^3)	18.50	15.41	15.47	16.41	20.75
Initial void ratio e_{init}	0.50	2.13	2.10	1.95	0.57
Mean SPT N_{30}	-	1	3	6	20
Undrained Shear Strength S_u (kPa)	0	17	29	37	0
Cohesion c' (kPa)	5.00	6.55	11.04	10.05	2.20
Friction angle φ' (deg)	20.00	24.28	25.46	27.38	31.50
Dilation angle ψ (deg)	0.0	0.0	0.0	0.0	1.5
Secant stiffness E_{ref}^{50} (MPa)	10.0	-	-	-	44.0
Tangent stiffness E_{ref}^{oed} (MPa)	10.0	-	-	-	44.0
Unloading stiffness E_{ref}^{ur} (MPa)	30.0	-	-	-	132.0
Power for stress dependency m	0.50	1.00	0.98	0.96	0.55
Unloading Poisson's ratio ν_{ur}	0.20	0.15	0.15	0.15	0.2
Compression index C_c	-	0.949	0.849	0.866	-
Swelling index C_s	-	0.104	0.077	0.075	-
Creep index $C_\alpha = 0.038C_c$	-	0.036	0.032	0.033	-
Radial permeability k_x, k_y (m/day)	1	5.84E-5	1.65E-6	2.74E-4	5E-3
Vertical permeability k_z (m/day)	1	2.92E-5	8.25E-7	1.37E-4	5E-3
Interfaces R_{inter}	0.8	0.7	0.7	0.7	0.8

Additionally, the boundary conditions for deformation are taken as follows: four faces on side boundaries are normally fixed, the bottom face is fully fixed, and the top surface is free. Regarding the boundary conditions for groundwater flow, the top surface is open as the water flows freely across it, while the remaining faces are closed, meaning that zero Darcy flux over the boundaries.

4. Results and Discussion

4.1. Convergence of the Numerical Model

The finite element mesh should be sufficiently small to ensure the reliability of the numerical results. However, the mesh refinement should cease as soon as further refinement has negligible impact on the results while significantly increasing the computational workload. To determine the optimal mesh configuration, analyses were performed for the models being discretized with fine and very fine meshes, as shown in Figure 4. The fine mesh and very fine mesh models comprise 119295 and 123175 soil elements, respectively.

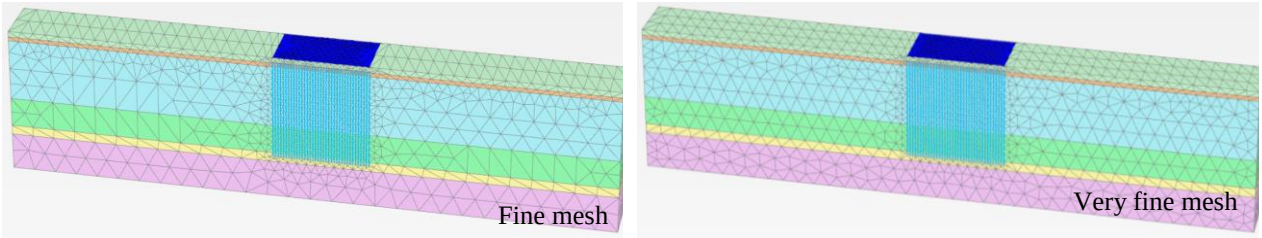

Figure 4. The 3D numerical models with fine and very fine meshes

The surface ground settlement at point S0 obtained from two models is shown in Figure 5. Obviously, the results are almost identical, indicating the sufficient mesh convergence and the reliability of the numerical results. Accordingly, the fine mesh discretization was chosen for the subsequent analyse.

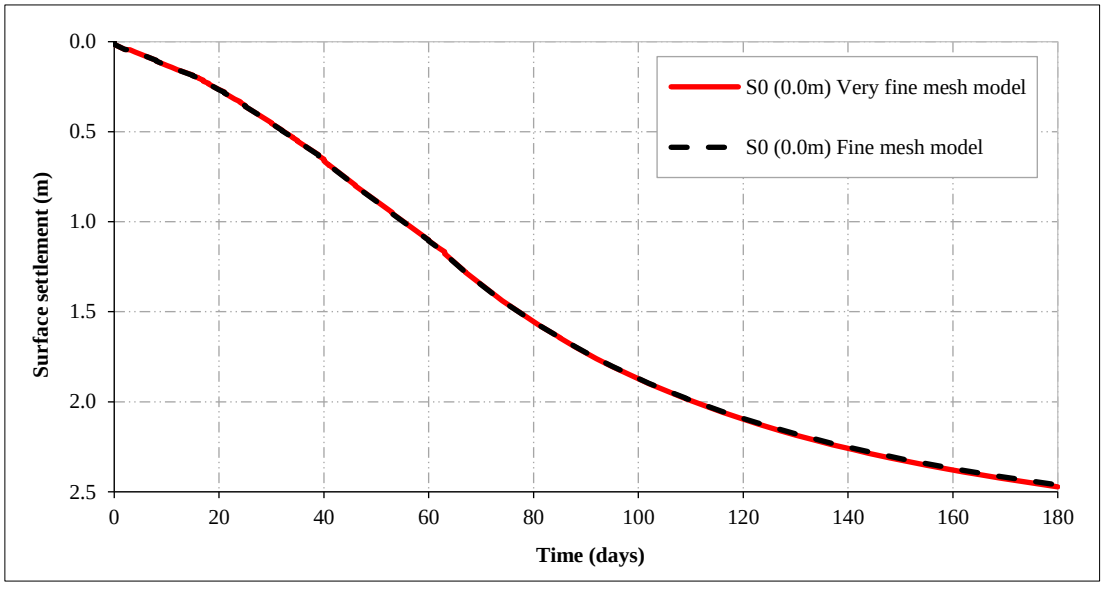

Figure 5. The surface ground displacement obtained by models with fine and very fine meshes

4.2. Ground Settlement

The results of the 3D FEM model are validated with the field measured data. Figure 6 shows the history of preloading pressure and soil settlements obtained from numerical simulations and field observation. The settlements were recorded at ground surface and at the depth of -4.8 m, -14.4m, and -24.4m. These locations are represented by points S0, S1, S2, and S3, as shown in Figure 3. Overall, the trend and magnitude of ground settlements estimated by the FEM models are in good agreement with those of monitoring data. The root mean squared errors (RSME) between the simulated and observed settlements are 0.14, 0.11, 0.06, and 0.09 m for S0, S1, S2, and S3, respectively. In the field of geotechnical engineering with many uncertainties in soil profiles, these figures are sufficiently accurate, proving the fidelity of the numerical models.

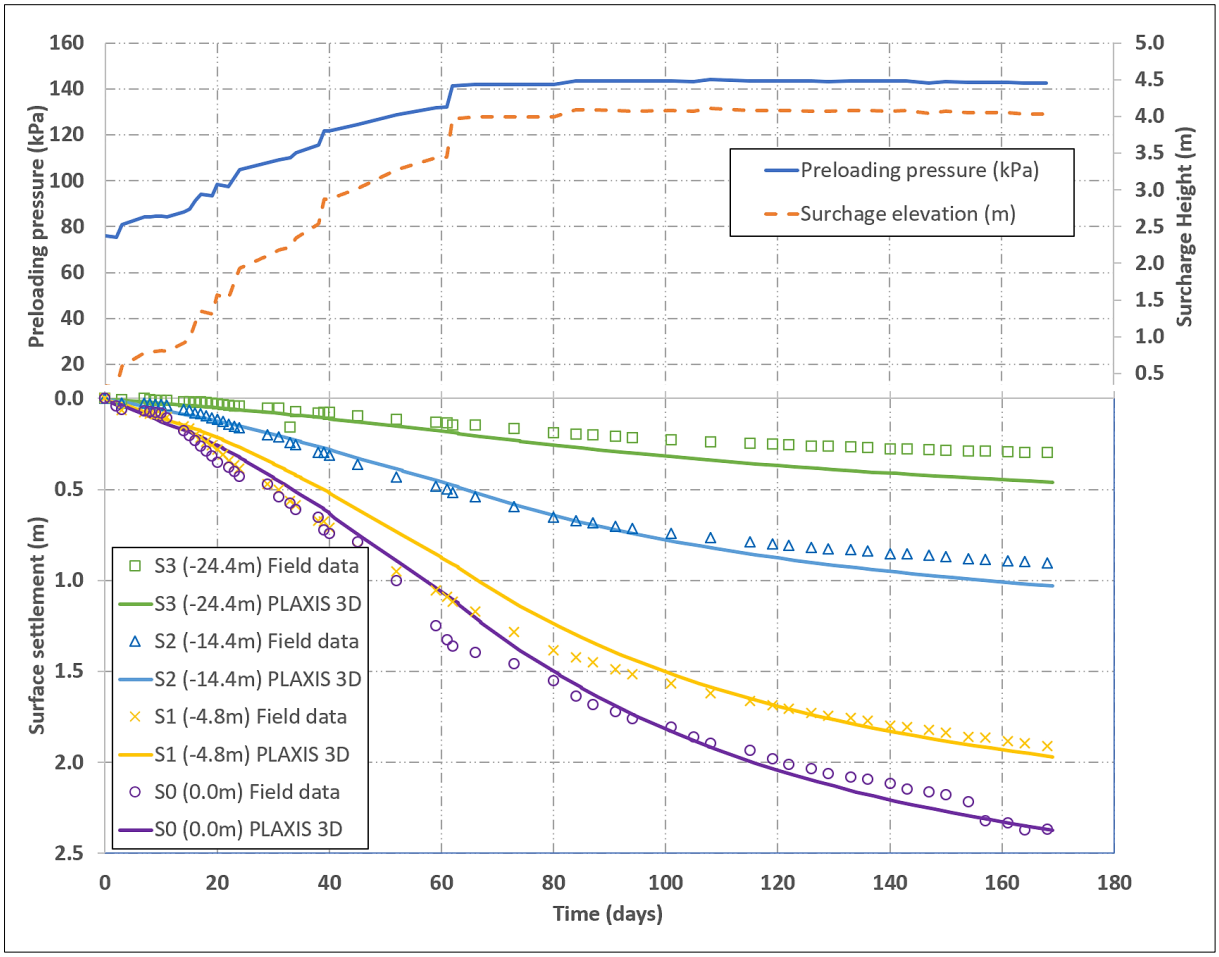

Figure 6. Settlements obtained from field data and FEM model

The 3D FEM effectively illustrates the settlement of the ground during consolidation, with significant influence from soil layers above -4.8m elevation. This is evident in both monitoring results and final simulation comparisons. The applied load primarily consolidates the upper layers first, while deeper layers experience less impact due to increasing self-weight stress. As shown in Figure 6, during the first 100 days, field monitoring showed a higher settlement rate at the points S0 and S1, compared to the simulation. However, at the points S2 and S3, the simulated settlements closely matched observational data. After 100 days, the simulation results at S0 and S1 aligned well with field data, with minimal discrepancies by the end of the process. In contrast, at the points S2 and S3, the simulation deviated further from actual results. The deviation at -14.4m was 14.025%, while at -24.4m, it reached 54.084%.

Regarding the rate of the consolidation process, the settlements were faster in the 60-day loading process, with increasing vacuum and surcharge loading pressures. In the next 110 days, there was a gradual increase in settlement while the loading pressures were kept constant. The settlement rate at the ground surface of the former period was about 2.1 times faster than that of the latter period. Bergado et al. reported a similar trend while investigating a project in which soft Bangkok clay was improved with surcharge and vacuum preloading [32]. In their work, the observed and simulated ground surface settlements at Zone 2 of the project showed that the settlement rates during loading process were about 2.3 times faster than that of the period with constant pressure.

Besides, an 3D FEM analysis was performed to estimate the final consolidation settlements, i.e. the settlement at the end of consolidation process when EPWP is dissipated completely. The final consolidation settlement at the point S0 was 4.618 m. For comparison purpose, this settlement value was also calculated using experimental data of 1D conventional oedometer test, as follows

$$S = \frac{C_s}{1+e_0} H \log\left(\frac{\sigma_p}{\sigma'_1}\right) + \frac{C_c}{1+e_0} H \left(\frac{\sigma'_1+\Delta\sigma}{\sigma_p}\right) \quad (5)$$

where C_s is the swelling index, C_c is the compression index, e_0 is the initial void ratio, H is the thickness of the soft clay layer, σ_p is the pre-consolidation pressure, σ'_1 is the effective vertical stress at the middle of the soft soil layer before vacuum-surcharge loading, and $\Delta\sigma$ is the applied pressure of vacuum-surcharge loading. With $C_s = 0.104$, $C_c = 1.000$, $e_0 = 2.130$, $H = 32.7$ m, $\sigma_p = 100$ kPa, $\sigma'_1 = 90.4$ kPa, and $\Delta\sigma = 145$ kPa, the value of S is 4.341 m. The result of the numerical model agrees well with this number, with a difference of around 6%.

4.3. Lateral Displacement

Figure 7 presents the simulated lateral displacement profile at the toe of the surcharge embankment at the end of the vacuum-surcharge preloading process. Negative values of the displacement imply inward movements with soil moving toward the center of the surcharge embankment, while positive values denote outward movements.

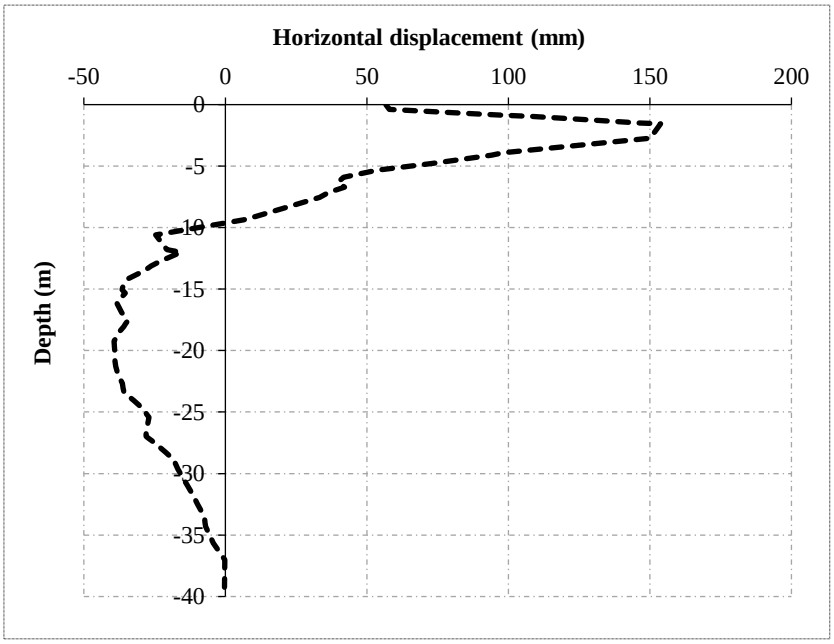

Figure 7. Lateral displacement profile at the toe of the surcharge embankment at 170 days

In general, the lateral displacement is considerable at the ground surface, around 50 mm. It keeps increasing until reaching the maximum value of around 150 mm at the depth of 1.55 m, followed by a gradually decrease. At the depth below 10 m, negative values of displacement indicate that the soil mass moves toward the center of preloading zone. A similar variation pattern of the lateral displacement was reported in the work of Long et al. [33]. They investigated an expressway project, located also in Nhon Trach, Dong Nai, Vietnam, nearby the project in this study. The soft clay treated with PVDs and vacuum-surcharge preloading at C1 section experienced a similar trend of lateral displacement, where the displacement increased from 125 mm at ground surface to the maximum 260 mm at the depth of 1 m, followed by a gradual decrease with increasing depth. Besides, Chai et al. showed similar patterns when they analyzed the lateral displacements of a runway and taxi road construction at Bangkok International Airport, denoted as case 3-5 in their paper [34].

The depth at which maximum lateral displacement occurs can be explained by the potential slip planes of the soil profile. A safety analysis phase using shear strength reduction method combined with FEM was performed after the end of preloading process, e.g. at 170 days. Figure 8 shows the potential slip planes, in which the shallow depth around the embankment toe experiences larger lateral displacements. Consequently, the maximum lateral displacement may occur along the shallow-depth slip plane.

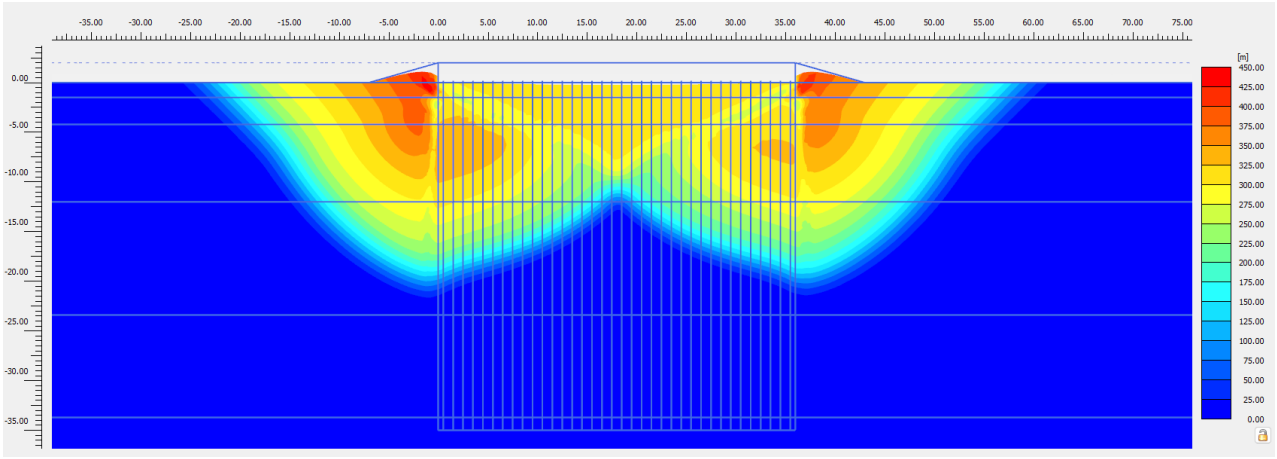

Figure 8. Potential slip plane

4.4. Excess Pore Water Pressure

Figure 9 shows the PWP measured at the depth of -5.5m, -15.5m, and -25.5m. Overall, the variation trends of PWP obtained by the FEM models are reasonable in comparison with the field data. Both numerical and field data show that the PWP increases during the first 60 days and gradually decreases in the next 110 days. This tendency is directly related to the loading process, in which the vacuum-surcharge preloading pressure were accumulated for the first 60 days and were kept at a constant level in the next period of time.

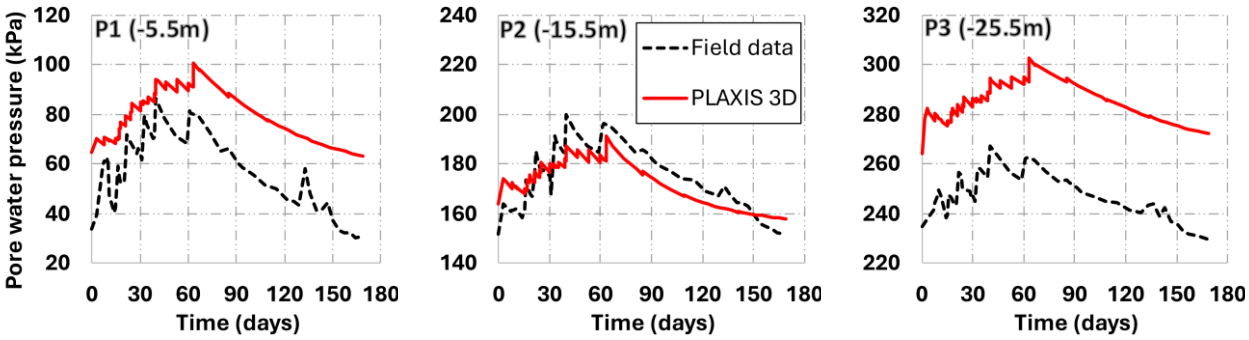

Figure 9. Pore water pressure obtained from field data and FEM model

In contrast, the PWPs measured on-site at point P1 and point P3 are considerably lower than their numerical counterparts. It could be explained by the loss of pressure during the vacuum process, which cannot be captured in numerical simulation. Nevertheless, it is the EPWP, not the PWP itself, that plays a critical role in the consolidation phenomenon of soft soil. The EPWP is the increment of the PWP compared with its original steady state, due to the vacuum-surcharge preloading. In Figure 9, it is observed that the rate of increase or decrease in PWP, i.e. the slope of the graphs, is almost identical in both field observation and numerical results.

There is a strong correlation between the ground settlement and the dissipation of EPWP. As shown in Figure 6, there is a fast increase in ground settlement in the process of loading during the first 60 days, followed by a gradual increase in the next 110 days as a result of consolidation. Meanwhile, in the first 60 days, the EPWP increases, as the pore pressure accumulates in the loading process. In the next 110 days, the EPWP keeps dissipating and transferring the stress to the soil skeleton. Therefore, the ground continues to settle despite that the preloading pressure levels off.

In Figure 10, the EPWP field is plotted at different elapsed time to better visualize the flow and drainage path of water. The excess pressure is only accumulated in the clay due to low permeability, while it is zero in the highly permeable sand layer, meaning that EPWP dissipates almost immediately after loading. Besides, it can be clearly observed that the EPWP gradually increases from 2 to 63 days, corresponding to the loading procedure, while decreasing with time in the consolidation process. The decrease in EPWP mainly occurs in the zone improved with PVDs. In contrast, the EPWP in the soil region without PVDs remains nearly unchanged at 63, 127, and 179 days. This observation evidently shows the effectiveness of PVDs in increasing the permeability and accelerating the consolidation process of soft soil.

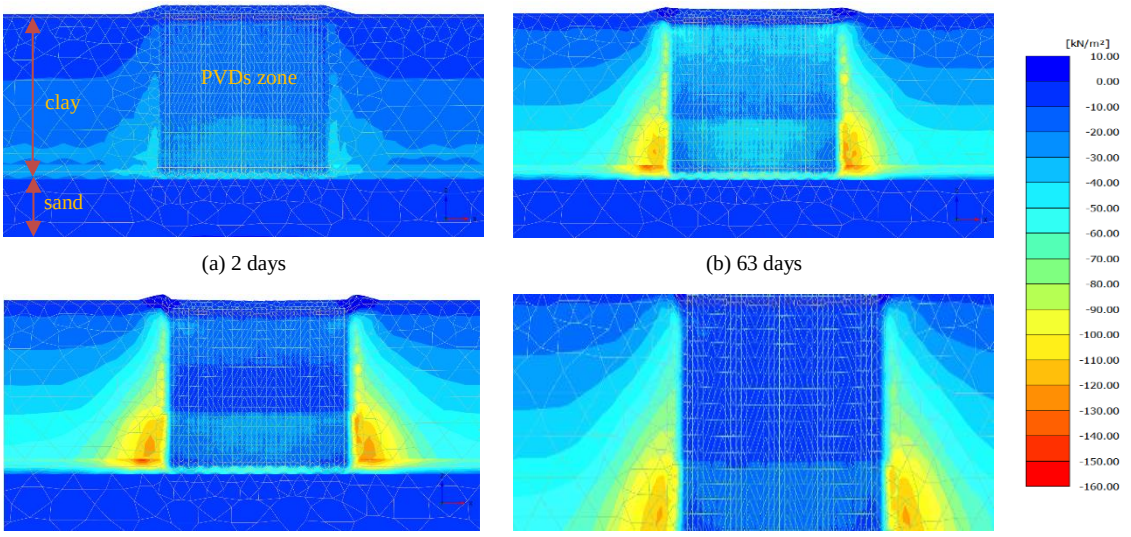

(a) 2 days (b) 63 days

(c) 127 days (d) 179 days

Figure 10. Excess pore water pressure at different elapsed times

4.5. Coefficient for Equivalent Permeability in 2D Model for Soft Silty Clay in Dong Nai port

In large-scale projects where 3D simulations are computationally prohibited, plane strain 2D simulations can be feasible surrogates. However, to achieve a same degree of consolidation with 3D model, the 2D model should use calibrated horizontal permeabilities for the PVDs-treated and original clay layer, which accounts for the transformation from axisymmetric to plane-strain conditions.

In this study, given the field data of the ground-surface displacement history, back analysis was conducted to determine appropriate values of horizontal permeability for original and PVDs-treated silty clay in plane strain model. By alternating the horizontal permeability of clay layer in 2D plane strain setting k_{hp} and comparing the numerical and observed displacements at ground surface, proper values of the plane-strain permeability can be selected. Let k_h be the horizontal permeability of clay layer in 3D axisymmetric model. The conversion ratio is defined as $\alpha = k_h/k_{hp}$. Figure 11 shows the settlement at ground surface, calculated by PLAXIS 2D using different values of conversion ratio α. Also, the corresponding field data is plotted to evaluate the results of 2D models. Obviously, the value of α within the range from 1.872 to 4.538 produces better results which closely agree with the field observations for the soft silty clay in Dong Nai Port.

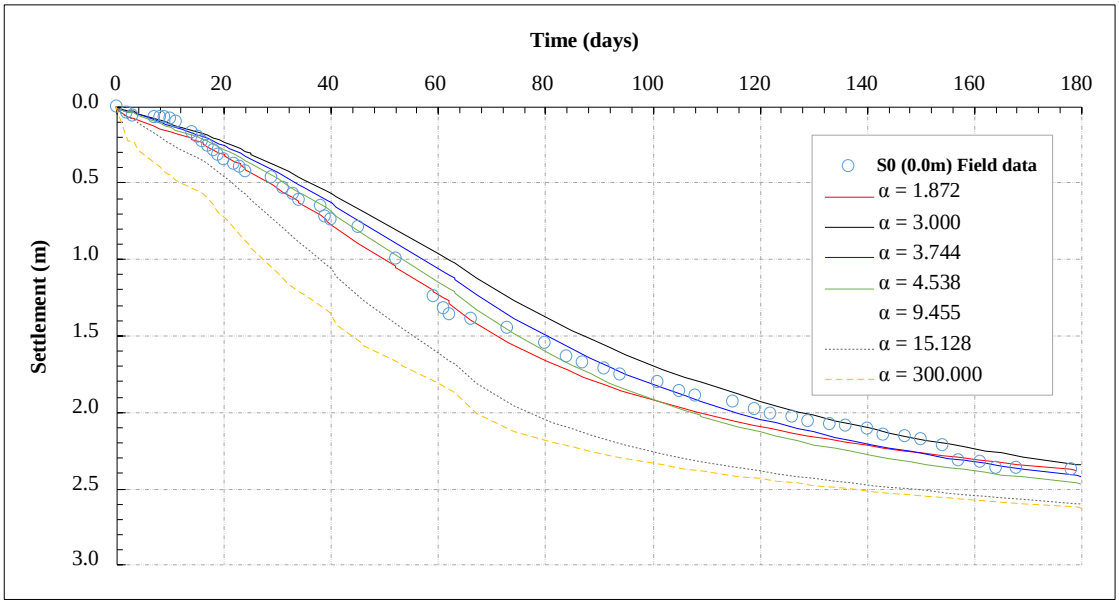

Figure 11. Ground surface displacement obtained from field data and 2D FEM model using different values of α

Indraratna et al. proposed a formula to calculate the equivalent plane strain horizontal permeability from its axisymmetric counterpart [14], expressed as

$$\frac{k_{hp}}{k_h} = \frac{\frac{2}{3}\left(1-\frac{1}{n}\right)^2}{ln\, n - 0.75} \tag{6}$$

where n is the spacing ratio. The spacing ratio is calculated as $n = D_e/d_w$, where D_e is the diameter of the unit cell and d_w is the equivalent diameter of drain. For square pattern of PVDs, $D_e = 1.13s$ in which s is the spacing between drains [35]. The equivalent diameter of drain is taken as $d_w = 2(a+b)/\pi$ in which a and b are the width and thickness of band drain, respectively [36]. In this project, the properties of the PVDs were taken as $a = 0.1$ m, $b = 0.004$ m, and $s = 1.0$ m. Using Equation (6), the ratio k_{hp}/k_h was obtained as 0.283, leading to the conversion ratio $\alpha = k_h/k_{hp} = 3.533$. Obviously, the back-analysis results, with α ranging from 1.872 to 4.538, are within the same order of magnitude.

Figure 12 shows the ground settlement at different depths, namely -4.8 m, -14.4 m, and -24.4 m, estimated by 2D model, before and after the permeability calibration using conversion ratio α = 1.872. Without the calibration, the settlements at deeper points S2 and S3 match those from field data, but the settlement at shallow depth S1 deviates substantially from the field measurement. The calibration clearly improves the settlement prediction, in which the projected settlements of all points are in good agreement with the field data.

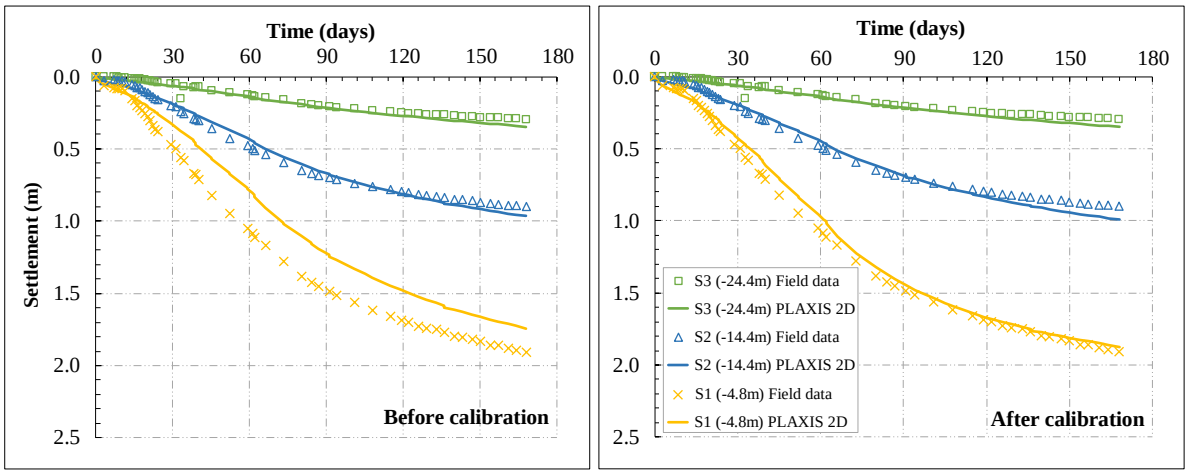

Figure 12. Ground settlement at S1, S2, and S3 calculated by PLAXIS 2D before and after permeability calibration

4.6. Optimum Length of PVDs

When vacuum pressure and surcharge embankment are applied directly to the soft ground, the pore water pressure initially increases. Subsequently, as water dissipates, the soil skeleton is compressed, leading to ground settlement. This consolidation process occurs not only within the treated area but also in adjacent zones and beneath the tips of the PVDs. As mentioned in the introduction section, there exists an optimum length of PVDs that accelerates the consolidation as effective as the longer PVDs while minimizing construction costs.

Normally, the PVDs are installed up to the full depth of soft soil layer. However, stresses induced by vacuum-surcharge preloading diminish with depth, thus the drains are not likely to accelerate the consolidation if the increased stress is smaller than a threshold. In the Dong Nai port area, where the silty soft clay layer extends to a depth of approximately 37 meters, fully penetrating PVDs throughout the entire weak soil profile is economically inefficient. This is because deep PVD installation does not substantially enhance the rate of consolidation or settlement acceleration, resulting in excessive material consumption and labor costs without a corresponding improvement in ground stabilization efficiency. By analyzing the surface settlement with respect to PVDs installation depth, it is possible to determine the optimum length of PVDs. Figure 13 shows the ground surface settlement predicted by numerical model in different cases of PVDs length. In case of 35 m length of PVDs, the speed of consolidation is slightly faster than that in case of 28 m length, which is as expected. Nonetheless, it is only a marginal increase, and the 28 m length option should be selected because of its cost-effectiveness.

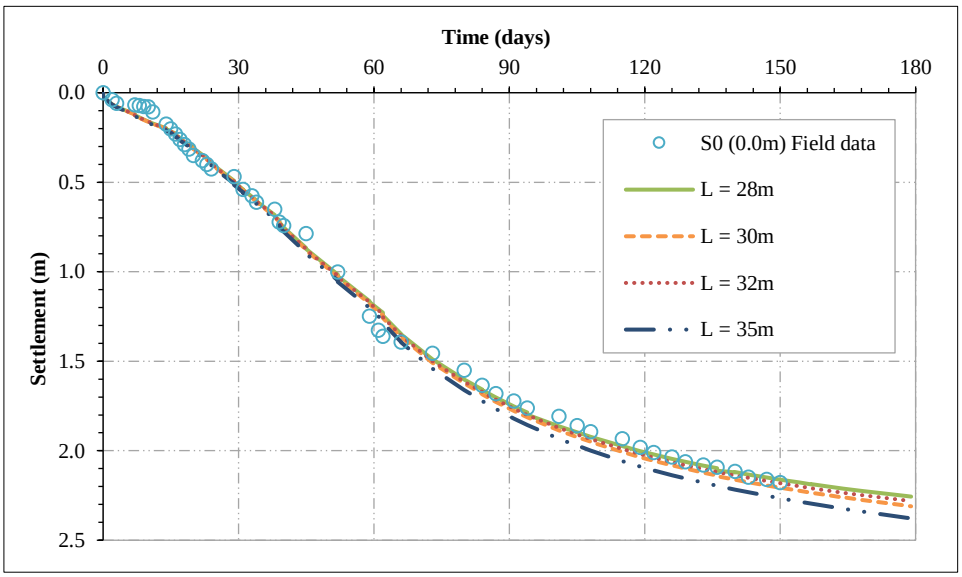

Figure 13. Soil surface settlement in different cases of PVDs length

In this project, the optimum length of PVDs is 28 m, which is around 76% of PVDs length fully-penetrated into 37 m thick layer of soft soil. This percentage is comparable to that of several published documents. Chai et al. reported an optimum PVDs length of 9.3 m in a 11 m thick layer of silty clay in Saga, Japan, accounting for about 85% of the fully-

penetrated length [9]. Meanwhile, Chen et al. studied an embankment loading on a soil profile consisting 15 m of soft silty clay in Jiangxi, China and suggested the optimum length of PVDs being taken from 10 to 12.8 m, meaning 67% to 85% of the full penetration [22].

5. Conclusion

This paper analyzes a port project in Dong Nai, Vietnam, in which a 37 m thick layer of very soft to soft soil was treated with PVDs and vacuum-surcharge preloading, using field observational data and FEM numerical simulations with consolidation theory. It has been demonstrated that: (i) the trend and magnitude of the ground settlements obtained by 3D FEM model are in good agreement with those of field data, with the root mean squared errors ranging from 0.06 to 0.14 m, (ii) the settlement rate in the 60-day increasing preloading pressure is about 2.1 time faster than that in the subsequent 110 days with constant preloading pressure, (iii) at 170 days, the lateral displacement at the embankment toe is around 50 mm at the ground surface, increasing with depth and reaching its maximum value of 150 mm at the depth of 1.55 m, (iv) the variation of pore water pressure is directly related to the preloading process and strongly correlated with the settlement rate, in which the pressure increases during the first 60 days and gradually dissipates in the next 110 days, (v) the back analysis of the ground surface displacement indicates that a 3D-to-2D conversion ratio of permeability ranging from 1.872 to 4.538 should be applied to acquire a same degree of consolidation between axisymmetric and plane-strain models, and (vi) a PVDs length of around 28 m is optimum for this project, which is 76% of the fully-penetrated length into soft clay layer. However, it should be noticed that although these specific values of permeability conversion ratio and optimum PVDs length are successfully applied to this project, these figures are case-specific and based on back analysis. For different soil profiles, further investigation should be conducted.

6. Declarations

6.1. Author Contributions

Conceptualization, K.T.N. and N.T.L.; software, T.M.N.; formal analysis, T.M.N.; resources, K.T.N.; writing—original draft preparation, T.M.N. and N.T.L.; writing—review and editing, T.M.N. and K.T.N.; visualization, T.M.N.; supervision, K.T.N. and N.T.L. All authors have read and agreed to the published version of the manuscript.

6.2. Data Availability Statement

The data presented in this study are available on request from the corresponding author.

6.3. Funding and Acknowledgements

We acknowledge Ho Chi Minh City University of Technology (HCMUT), VNU-HCM for supporting this study.

6.4. Conflicts of Interest

The authors declare no conflict of interest.

7. References

[1] Knappett, J., & Craig, R. F. (2019). Craig's Soil Mechanics. In Craig's Soil Mechanics. doi:10.1201/9781351052740.

[2] Shukla, S. K., Sivakugan, N., & Das, B. M. (2009). Methods for determination of the coefficient of consolidation and field observations of time rate of settlement-An overview. International Journal of Geotechnical Engineering, 3(1), 89–108. doi:10.3328/IJGE.2009.03.01.89-108.

[3] Abeele, W., Nyhan, J. W., Hakonson, T. E., Drennon, B. J., Lopez, E. A., Herrera, W. J., ... & Trujillo, G. (1986). Consolidation and shear failure leading to subsidence and settlement. Final report (No. LA-10576-MS), Los Alamos National Lab (LANL), Los Alamos, United States. doi:10.2172/6082905.

[4] Vinoth, M. (2025). Ground Improvement by Prefabricated Vertical Drains and Surcharge for a Metro Depot Constructed on Marine Deposit. Transportation Infrastructure Geotechnology, 12(3), 1–38. doi:10.1007/s40515-025-00574-z.

[5] Bergado, D. T., Jamsawang, P., Voottipruex, P., Jongpradist, P., Rementilla, J., & Dicker, S. (2024). First and second vacuum-PVD improvement of soft Bangkok clay for the third runway of Suvarnabhumi International Airport Thailand. Innovative Infrastructure Solutions, 9(9), 348. doi:10.1007/s41062-024-01669-1.

[6] Liu, K., He, H. T., Tan, D. Y., Feng, W. Q., Zhu, H. H., & Yin, J. H. (2024). A Case Study of Performance Comparison Between Vacuum Preloading and Fill Surcharge for Soft Ground Improvement. International Journal of Geosynthetics and Ground Engineering, 10(1), 11. doi:10.1007/s40891-024-00521-x.

[7] Feng, S., Bai, W., Lei, H., Song, X., Liu, W., & Cheng, X. (2024). Vacuum preloading combined with surcharge preloading method for consolidation of clay-slurry ground: A case study. Marine Georesources & Geotechnology, 42(4), 348–361. doi:10.1080/1064119X.2023.2185843.

[8] Wu, J., Xuan, Y., Deng, Y., Li, X., Zha, F., & Zhou, A. (2021). Combined vacuum and surcharge preloading method to improve lianyungang soft marine clay for embankment widening project: A case. Geotextiles and Geomembranes, 49(2), 452–465. doi:10.1016/j.geotexmem.2020.10.013.

[9] Chai, J. C., Carter, J. P., & Hayashi, S. (2006). Vacuum consolidation and its combination with embankment loading. Canadian Geotechnical Journal, 43(10), 985–996. doi:10.1139/T06-056.

[10] Barron, R. A. (1948). Consolidation of Fine-Grained Soils by Drain Wells by Drain Wells. Transactions of the American Society of Civil Engineers, 113(1), 718–742. doi:10.1061/taceat.0006098.

[11] Hansbo, S. (1981) Consolidation of Fine-Grained Soils by Prefabricated Drains. 10th International Conference on Soil Mechanics and Foundation Engineering, 15-19 June, 1981, Stockholm, Sweden.

[12] Shen, Z., Chian, S. C., Tan, S. A., & Leung, C. F. (2024). Modelling smear effect of vertical drains using a diameter reduction method. Journal of Rock Mechanics and Geotechnical Engineering, 16(1), 279–290. doi:10.1016/j.jrmge.2023.06.021.

[13] Hird, C. C., Pyrah, I. C., Russell, D., & Cinicioglu, F. (1995). Modelling the effect of vertical drains in two-dimensional finite element analyses of embankments on soft ground. Canadian Geotechnical Journal, 32(5), 795–807. doi:10.1139/t95-077.

[14] Indraratna, B., Sathananthan, I., Rujikiatkamjorn, C., & Balasubramaniam, A. S. (2005). Analytical and Numerical Modeling of Soft Soil Stabilized by Prefabricated Vertical Drains Incorporating Vacuum Preloading. International Journal of Geomechanics, 5(2), 114–124. doi:10.1061/(asce)1532-3641(2005)5:2(114).

[15] Parsa-Pajouh, A., Fatahi, B., Vincent, P., & Khabbaz, H. (2014). Trial Embankment Analysis to Predict Smear Zone Characteristics Induced by Prefabricated Vertical Drain Installation. Geotechnical and Geological Engineering, 32(5), 1187–1210. doi:10.1007/s10706-014-9789-9.

[16] Cheung, Y. K., Lee, P. K. K., & Xie, K. H. (1991). Some remarks on two and three dimensional consolidation analysis of sand-drained ground. Computers and Geotechnics, 12(1), 73–87. doi:10.1016/0266-352X(91)90012-5.

[17] Parsa-Pajouh, A., Fatahi, B., Vincent, P., & Khabbaz, H. (2014). Analyzing consolidation data to predict smear zone characteristics induced by vertical drain installation for soft soil improvement. Geomechanics and Engineering, 7(1), 105–131. doi:10.12989/gae.2014.7.1.105.

[18] Kan, M. E., Indraratna, B., & Rujikiatkamjorn, C. (2021). On numerical simulation of vertical drains using linear 1-dimensional drain elements. Computers and Geotechnics, 132, 103960. doi:10.1016/j.compgeo.2020.103960.

[19] Ong, C. Y., Chai, J. C., & Hino, T. (2012). Degree of consolidation of clayey deposit with partially penetrating vertical drains. Geotextiles and Geomembranes, 34, 19–27. doi:10.1016/j.geotexmem.2012.02.008.

[20] Chai, J. C., Miura, N., Kirekawa, T., & Hino, T. (2009). Optimum PVD installation depth for two-way drainage deposit. Geomechanics & Engineering, 1(3), 179–191. doi:10.12989/gae.2009.1.3.179.

[21] Vu, V. T. (2015). Optimal Layout of Prefabricated Vertical Drains. International Journal of Geomechanics, 15(3), 6014020. doi:10.1061/(asce)gm.1943-5622.0000434.

[22] Chen, J., Shen, S. L., Yin, Z. Y., Xu, Y. S., & Horpibulsuk, S. (2016). Evaluation of Effective Depth of PVD Improvement in Soft Clay Deposit: A Field Case Study. Marine Georesources & Geotechnology, 34(5), 420–430. doi:10.1080/1064119X.2015.1016638.

[23] PORTCOAST. (2021). Phuoc An Port and Logistics service area project (Phase 1), Construction Design Documents, Dong Nai Province, Vietnamese.

[24] PORTCOAST. (2021). Phuoc An Port and Logistics service area project (Phase 1), Soil Investigation Report, Dong Nai Province, Vietnamese.

[25] PLAXIS. (2023). PLAXIS 3D Manuals CONNECT Edition. Bentley Systems Inc., Pennsylvania, United States.

[26] Biot, M. A. (1956). General Solutions of the Equations of Elasticity and Consolidation for a Porous Material. Journal of Applied Mechanics, 23(1), 91–96. doi:10.1115/1.4011213.

[27] Architectural Institute of Japan (AIJ). (2001). Recommendations for design of building foundations. Architectural Institute of Japan (AIJ), Tokyo, Japan. (In Japanese).

[28] Mesri, G., Stark, T. D., Ajlouni, M. A., & Chen, C. S. (1997). Secondary Compression of Peat with or without Surcharging. Journal of Geotechnical and Geoenvironmental Engineering, 123(5), 411–421. doi:10.1061/(asce)1090-0241(1997)123:5(411).

[29] Holtz, R. D., Jamiolkowski, M. B., Lancellotta, R., and Pedroni, R. (1991). Prefabricated vertical drains: design and performance. Butterworth-Heinemann, Oxford, United Kingdom.

[30] Bo, M.W., Chu, J., Low, B.K. and Choa, V. (2003) Soil Improvement: Prefabricated Vertical Drain Technique. Thomson Learning, Singapore.

[31] Hansbo, S. (1997). Aspects of vertical drain design: Darcian or non-Darcian flow. Geotechnique, 47(5), 983–992. doi:10.1680/geot.1997.47.5.983.

[32] Bergado, D. T., Jamsawang, P., Jongpradist, P., Likitlersuang, S., Pantaeng, C., Kovittayanun, N., & Baez, F. (2022). Case study and numerical simulation of PVD improved soft Bangkok clay with surcharge and vacuum preloading using a modified air-water separation system. Geotextiles and Geomembranes, 50(1), 137–153. doi:10.1016/j.geotexmem.2021.09.009.

[33] Long, P. V., Bergado, D. T., Nguyen, L. V., & Balasubramaniam, A. S. (2013). Design and performance of soft ground improvement using PVD with and without vacuum consolidation. Geotechnical Engineering, 44(4), 36–51. doi:10.14456/seagj.2013.5.

[34] Chai, J., Ong, C. Y., Carter, J. P., & Bergado, D. T. (2013). Lateral displacement under combined vacuum pressure and embankment loading. Geotechnique, 63(10), 842–856. doi:10.1680/geot.12.P.060.

[35] Rixner, J. J., Kraemer, S. R., & Smith, A. D. (1986). Prefabricated Vertical Drains, Vol. I, II and III: Summary of Research Report-Final Report. Federal Highway Admin., Report No. FHWA-RD-86/169, Washington, United Kingdom.

[36] Hansbo, S. (1979). Consolidation of Clay By Band-Shaped Prefabricated Drains. Ground Engineering, 12(5), 16–18, 21. doi:10.1016/0148-9062(80)90141-2.